Printed in the Republic of Korea

ANALYTICAL SCIENCE & TECHNOLOGY

Vol. 29 No. 1, 35-42, 2016

http://dx.doi.org/10.5806/AST.2016.29.1.35

A new nano-composite carbon ink for disposable dopamine biosensors

T. Dinakaran and S.-C. Chang[1,★]

Graduate Department of Chemical Materials, Pusan National University
[1]Institute of Bio-Physio Sensor Technology, Pusan National University, 2 Busandaehak-ro, Geumjeong-gu, Busan 46241, Korea

(Received January 26, 2016; Revised February 10, 2016; Accepted February 11, 2016)

나노컴포지트 카본 잉크가 전착된 일회용 도파민 바이오센서

띠루 디나카란 · 장승철[1,★]

부산대학교 화학소재학과(대학원), [1]부산대학교 바이오피지오센서연구소

(2016. 1. 26. 접수, 2016. 2. 10. 수정, 2016. 2. 11. 승인)

Abstract: A new nano-composite carbon ink for the development of disposable dopamine (DA) biosensors based on screen-printed carbon electrodes (SPCEs) is introduced. The method developed uses SPCEs coupled with a tyrosinase modified nano-composite carbon ink. The ink was prepared by an "in-house" procedure with reduced graphene oxide (rGO), Pt nanoparticles (PtNP), and carbon materials such as carbon black and graphite. The rGO-PtNP carbon composite ink was used to print the working electrodes of the SPCEs and the reference counter electrodes were printed by using a commercial Ag/AgCl ink. After the construction of nano-composite SPCEs, tyrosinase was immobilized onto the working electrodes by using a biocompatible matrix, chitosan. The composite of nano-materials was characterized by X-ray photoelectron spectroscopy (XPS) and the performance characteristics of the sensors were evaluated by using voltammetric and amperometric techniques. The cyclic voltammetry results indicated that the sensors prepared with the rGO-PtNP-carbon composite ink revealed a significant improvement in electro-catalytic activity to DA compared with the results obtained from bare or only PtNP embedded carbon inks. Optimum experimental parameters such as pH and operating potential were evaluated and calibration curves for dopamine were constructed with the results obtained from a series of amperometric detections at -0.1 V *vs.* Ag/AgCl. The limit of detection was found to be 14 nM in a linear range of 10 nM to 100 μM of DA, and the sensor's sensitivity was calculated to be 0.4 $\mu A \mu M^{-1} cm^{-2}$.

Key words: reduced graphene oxide, nano-composite, screen printed carbon electrode, dopamine, tyrosinase, biosensor

★ Corresponding author
Phone : +82-(0)51-510-2276 Fax : +82-(0)51-514-2122
E-mail : s.c.chang@pusan.ac.kr

1. Introduction

Dopamine (3,4-dihydroxyphenylethylamine, DA) is a catecholamine neurotransmitter in mammalian central nervous systems (CNS), plays significant role to modulate the variety of brain circuitry and hormonal systems. However, its abnormal level in CNS stimulates numerous neurological disorders, especially Parkinson's disease and schizophrenia.[1] Therefore, various analytical techniques have been introduced for the dopamine detection.[2] Among them, chromatographic techniques have been widely used such as GC-MS,[3] LC-MS,[4] LC with fluorescence detection,[5] LC with electrochemical (EC) detection[6] and flow injection analysis with chemiluminescence.[7] Although these methods achieved high sensitivity and selectivity, they usually required expensive equipment, highly trained technicians, slow turn-around time and complicated sample pretreatment steps. In order to overcome these problems, electrochemical techniques could be suggested as a convenient technique for the DA detection.[8]

It is well known that DA can be easily oxidized electrochemically at the surface of conventional electrodes. Some modified electrodes can be employed for *in vitro* or *in vivo* DA analysis.[9] However, those electrochemical approaches show some problems in analyses of biological or clinical samples. The DA concentration in the extracellular fluid of the caudate nucleus from normal persons typically range from 10 nM to 1.0 μM and the DA level from Parkinson's disease patients is as low as just a few nanomolar range,[10] which sometimes caused a poor signal to noise ratio (S/N) characteristics. In addition, the concentration level of major interference in biological or clinical samples including ascorbic acid (AA), ranges from 100 μM to 500 μM and these interference can be oxidized at nearly the same oxidizing potential of DA, which resulting in overlapped voltammetric responses.[11] To overcome these problems, the working electrodes in EC DA detection systems have been carefully elaborated with new nano or functional electrode materials such as graphite,[12] boron-doped diamond,[13] carbon nanofibers,[14] carbon nanotubes[15] and graphene based materials.[16] The different properties of each type of electrodes bound its own advantages and drawbacks. Therefore, it is still highly desired to explore novel electrode for detection of DA in the presence of AA.

In recent years, newly developed nano or functional materials have been applied to develop screen printed carbon electrodes (SPCEs) for the detection of DA.[17-19] Iridium oxide electrodeposited SPCE,[20] carbon nanotubes modified SPCE and graphene modified SPCE.[20] Among the carbon nanomaterials, graphene has obtained great attention in recent days due to their unique properties such as excellent electrical conductivity, high stability and large specific surface area. The selectivity enhancement of the SPCEs to DA could be easily achieved by using an enzyme, tyrosinase. In general, tyrosinase catalyzes the hydroxylation of phenols to catechols by cresolate activity and catechols to ortho-quinones by catecholase activity in the presence of molecular oxygen.[22] The enzymatically produced ortho-quinone could be reduced electrochemically to catechol at low potential without any mediators.[23] Following the same principle, DA, a catechol-like phenolic compound, could be detected by using tyrosinase based electrochemical biosensors.[24-26] A key technical issue for the tyrosinase modified SPCEs is an effective immobilization of tyrosinase onto the SPCE surface. Several immobilization approaches have been reported by using hydrogel,[27] sol-gel,[28] glutaraldehyde[29] and chitosan.[33]

In the present system, nano-composite carbon inks incorporated with chemically reduced graphene oxide (rGO) and platinum nanoparticles (PtNP) have been prepared to print SPCEs. To immobilize tyrosinase onto the SPCEs, a bio-polymer, chitosan, has been chosen as an enzyme modifier because of the polymer's good biocompatibility, film-forming properties, adhesion properties and robustness.[33] It is, therefore, suggested that the synergistic combination of the nano-composite carbon inks and tyrosinase can improve the sensor sensitivity and selectivity for the DA detection.

2. Experimental

2.1. Materials and Apparatus

Tyrosinase (E.C.1.14.18.1, from mushroom, 1000 U mg^{-1}), 8 wt.% of chloroplatinic acid (H_2PtCl_6), N,N-dimethyl formamide (DMF), chitosan, dopamine hydrochloride (DA), potassium phosphate monobasic (KH_2PO_4), sodium phosphate dibasic (Na_2HPO_4), ascorbic acid (AA), uric acid (UA), epinephrine (EP), norepinephrine hydrochloride (NorEP), serotonin hydrochloride (SR), 3,4-dihydroxy-L-phenylalanine (L-DOPA) and 3,4-dihydroxyphenyl acetic acid (DOPAC) were purchased from Sigma-Aldrich (USA). A commercial Ag/AgCl ink was from Gwent group Ltd. (UK). Carbon black (CB), Polyvinyl chloride (PVC) substrate, stencils, carbon ink, insulator ink and a commercial resin (G-2S) were purchased from Juju Chemical Co. Ltd. (Japan). All other chemicals were analytical grade and were used as received. All aqueous solutions were prepared in deionized water, which was obtained from a Milli-Q water purifying system (18 MΩ cm^{-1}). X-ray photoelectron spectroscopy (XPS) (Thermo Fisher Scientific, U.K.) was carried out at KBSI (Korea Basic Science Institute, Busan, South Korea). An amperometric and voltammetric measurements were carried out with an electrochemical workstation (Compactstat, Ivium Technologies, USA). Roller mixer was from Hwashin Technology Co., South Korea.

2.2. rGO and PtNP incorporated nano-composite carbon ink

Graphene oxide (GO) was synthesized from expanded graphite's according to a modified Hummers and Offeman method.[30-31] For reduction process, 1 g of the GO synthesized was sonicated in 1 L deionized water for 2 hours. A 10 mL aliquot of 32 mM hydrazine hydrate was added into the GO suspension and the solution was heated at 100 °C for 24 hours. After cooling, the suspension was filtered and washed several times with 95 % ethanol solution. The filtered platelets, chemically reduced GO (rGO), were then dried in vacuum oven at 80 °C for 12 h and re-suspended in DMF. To prepare the carbon ink, 1 mL aliquots of rGO, H_2PtCl_6 and 0.5 g of carbon black (CB) were dispersed into a 5.0 mL aliquot of DMF. The mixture was ultrasonically treated for several minutes and mixed for 24 h by a roller mixer. Consequently, the mixture was centrifuged at 2500 rpm for 5 min to remove the supernatant and was dried in an oven at 60 °C for 12 h to obtain the rGO-PtNP-CB nano-composite. For the comparison studies, only rGO-CB and only CB-PtNP composites were also prepared by using the same procedure. The dried nano-composite powders were then mixed with a commercial resin to form an ink with appropriate viscosity and stored at room temperature prior to use.

2.3. SPCE fabrication

Screen printed carbon electrodes (inset in Fig. 3) were fabricated on the PVC substrates by using a screen printer (BANDO industrial, model BS-450HT, South Korea). Three patterned stencils were used to make an Ag/AgCl conductive, a carbon layer and an insulating layers. The structure of the SPCE is consisting of a carbon ink printed electrode as a working electrode, an Ag/AgCl printed electrodes which serves as a reference and a counter electrode, respectively. An insulating layer was printed to cover the connection between the working electrode and the silver conductive layer, given the definite shape to the working electrode area (diameter: 3 mm). The rGO-PtNP-CB nano-composite was printed on the SPCEs to attain the rGO-PtNP-CB/SPCEs and CB/SPCEs, rGO-CB/SPCEs, CB-PtNP/SPCEs were also prepared. All SPCEs prepared were stored in the dark at room temperature prior to use

2.4. Enzyme immobilization

To immobilize the enzyme, tyrosinase, 6.4 $mg{\cdot}mL^{-1}$ tyrosinase solution was prepared in 0.1 M PBS (pH 6.5) and a 5 $mg{\cdot}mL^{-1}$ chitosan solution was prepared in 0.1 M acetic acid solution.[26] Chitosan and tyrosinase with a volume ratio of 1:2 were mixed thoroughly and 10 μL aliquots of the mixture were drop coated on the surface of working electrodes of rGO-PtNP-CB/SPCE. Then, enzyme modified electrodes were

allowed to dry at 4 °C for overnight and were gently rinsed with 0.1 M PBS (pH 7.2). The enzyme modified SPCEs were stored at 4 °C in the dark.

2.5. Measurement procedures

In order to investigate electrochemical behavior of DA, an electrochemical cell was set up using a 2 mL-volume disposable well with modified SPCEs and cyclic voltammetric experiments have been carried out. A 100 mL of 1 mM DA stock was prepared in 0.1 M PBS (pH 7.2) just before the measurements and the modified SPCEs were immersed in 1 mL aliquots of diluted DA solutions. After the 3-min incubation, cyclic voltammograms were obtained by potential sweeping from -0.6 V to 0.1 V *vs.* Ag/AgCl at a scan rate of 50 $m \cdot Vs^{-1}$. Amperometric measurements have also been performed by using the modified SPCEs. A modified SPCE was inserted into the electrochemical cell and connected to a potentiostat. A 900 µL aliquot of 0.1 M PBS was added to the well and the electrode was polarized at a potential of -0.1 V *vs.* Ag/AgCl. After achieving a stable baseline response with PBS, 100 µL samples of DA were added to the well and current responses as a function of time, were recorded. The measurement was repeated to construct calibration curves and each SPCE characteristics was investigated using the above procedure.

3. Results and Discussion

3.1. XPS analysis of nano-composite carbon inks

Three different nano-composite modified SPCEs were prepared by using the composite inks described in the section 2.3. In order to analyze the elemental composition of the elements that exist within the ink materials, XPS spectra of an rGO-PtNP-CB coated SPCE was constructed and was shown in Fig. 1. As can be seen in Fig. 1(A), a C 1s peak (284.6 eV), an O 1s peak (533.0) and a Pt 4f peak (72.5 eV) were observed. These peaks, apparently, confirm that the nano-composite carbon ink have carbon and Pt materials. Furthermore, the chemical and electronic

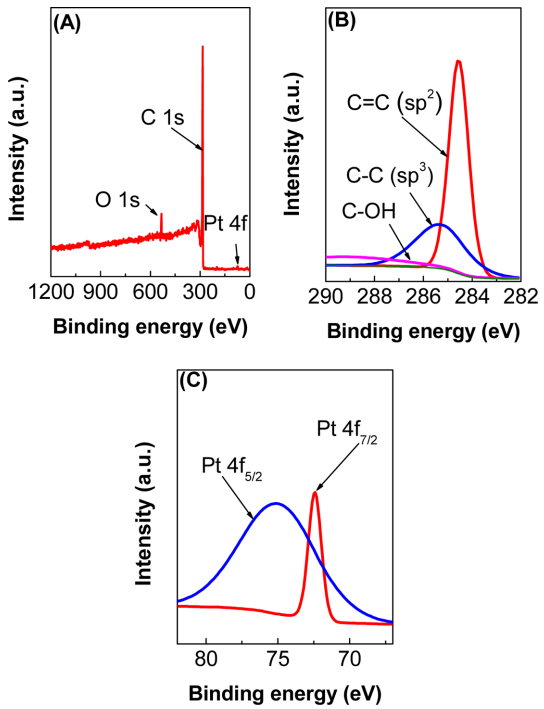

Fig. 1. XPS survey spectrum of rGO-PtNP-CB/SPCE (A), de-convoluted high resolution spectra of C 1s (B) and Pt 4f regions of rGO-PtNP-CB/SPCE (C). spectra of C 1s (B) and Pt 4f regions of rGO-PtNP-CB/SPCE (C).

states of the ink were evaluated by using the high resolution spectra at C 1s and Pt 4f regions. Fig. 1(B) shows the peaks at C 1s region and the peaks at binding energies of 284.5 eV, 285.3 eV and 289.1 eV, are corresponding to graphitic sp^2 (C=C), graphitic sp^3 (C-C) and hydroxyl (C-OH) groups, respectively. These peaks are well-known peaks of carbon materials, such as rGO and CB. The peak intensity of graphitic sp^2 higher than sp^3 and hydroxyl groups, and this confirms the maximum presence of rGO. Pt 4f region (Fig. 1(C)) shows doublet peaks at 72.4 eV (Pt $4f_{7/2}$) and 75.0 eV (Pt $4f_{5/2}$) are corresponding to metallic Pt^0. It clearly indicates the Pt nanoparticles presence in the nanocomposite and they are zero valence state. Therefore, these results confirm the successful reduction of H_2PtCl_6 to Pt^0 particles. It is also found that the doublet peaks are slightly shifted higher energy levels due to the interaction of Pt nanoparticles and rGO.[32] The XPS spectra obtained summarized in Table 1. Table 1 also

Table 1. Elemental content of nano-composites from XPS spectra

Nano-composites	Elements present (Atomic percentage)			Atomic ratio (C/O)
	C 1s	O 1s	Pt 4f	
CB	92.9	6.50	-	14.3
rGO-CB	89.1	9.50	-	9.40
CB-PtNP	88.1	9.50	0.20	9.30
rGO-CB-PtNP	94.6	4.10	0.20	23.1

shows an elemental composition of the nano-composites and atomic ratio of C/O obtained by XPS analysis. C/O ratio is important for improving nano-composites electrocatalytic activity, oxygen functional groups were significantly decreased and C-C interactions were increased in rGO-PtNP-CB/SPCE composite compared to other composites. It suggests that rGO-PtNP-CB/SPCE have an enhanced electro-catalytic activity.

3.2. Electrochemical response of different inks modified SPCE

Electrochemical performance characteristics of the modified SPCEs printed by using four different composite inks was investigated. Fig. 2(A) shows a comparative cyclic voltammograms of 100 μM DA in 0.1 M PBS (pH 7.2) on CB, CB-PtNP, rGO-CB and rGO-PtNP-CB coated SPCEs. As expected, no redox peaks are observed at these electrodes without tyrosinase. These indicate that no redox activity for DA in the selected potential range from -0.6 V to 0.1 V. However, in the case of tyrosinase modified

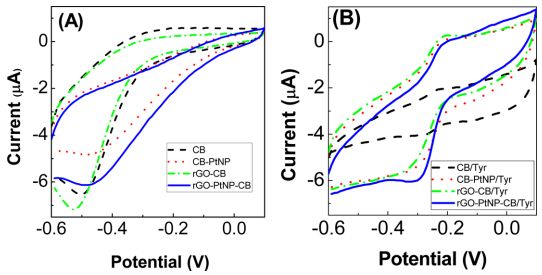

Fig. 2. Cyclic voltammograms for nanocomposite modified SPCEs without enzyme (A) and with immobilized enzyme, tyrosinase (B) in 0.1 M PBS (pH 7.2) containing 100 μM DA at a scan rate of 50 mVs^{-1}.

electrodes, clear reduction peaks were observed. These peaks could explain that the direct reduction of the enzymatically produced dopamine-o-quinone to its original form, DA. As can be seen in Fig. 2(B), the cyclic voltammograms of 100 μM DA at the CB/Tyr did not show well defined redox peaks because the bare CB did not have capability to reduce dopamine-o-quinone at the potential range applied. In the case of the CB-PtNP/Tyr electrode, however, an increased redox peak was observed. These results could explain that the Pt nanoparticles have significantly improved the electron transfer rate at the surface of the CB-PtNP/Tyr. Similar trend was observed at the rGO-CB/Tyr. A redox peak was found and the reduction peak was increased compared with the results of the CB-PtNP/Tyr, which ascribed the presence of rGO could enhance the electron transfer rate and a unique electrical conductivity. However, in the case of rGO-PtNP-CB/Tyr, the oxidation peak was slightly decreased; the reduction peak current value was increased compared with the results from rGO-CB/Tyr and was sharply shifted to the positive potential direction. These were obviously explained that the rGO with PtNP played an important role to improve the electron transfer between dopamine-o-quinone and the electrode surface. The cathodic peak current values (i_{pc}) were calculated from the results in Fig. 2 and the rGO-PtNP-CB/Tyr composite shows approximately 4.5 times higher i_{pc} values than CB/Tyr, 36 % points higher than PtNP-CB's and 11 % points higher than rGO-CB's, respectively. These results explain that the synergistic effect of the rGO-PtNP-CB composite clearly revealed an enhanced electro-catalytic activity of the composite as well as the high surface area-to-volume ratio of the composite, which could increase the amount of immobilized enzyme.

Amperometric measurement were carried out and the reduction current of enzymatically produced ortho-quinone were clearly occurred at a low applied potential of -0.1V *vs.* Ag/AgCl. A schematic representation of the overall reaction and a photo of SPCE is shown in Fig. 3. With immobilized tyrosinase, the current responses of four different nano-composite modified SPCEs to 100 μM DA were overlaid in

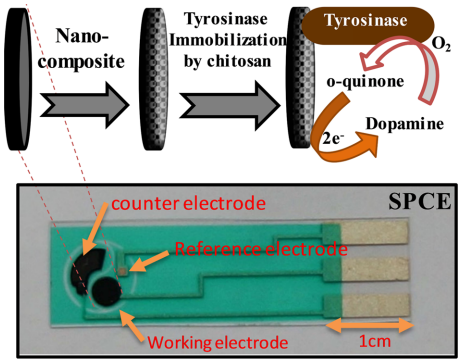

Fig. 3. Schematic representation of electrochemical detection of DA by using rGO-PtNP-CB/Tyr modified SPCEs.

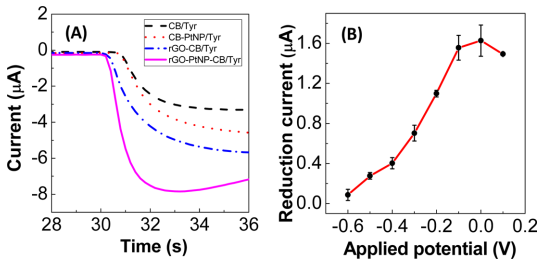

Fig. 4. Amperometric response of nano-composite modified SPCEs to 100 μM DA in 0.1 M PBS (pH 7.2) at applied potential of -0.1 V vs. Ag/AgCl. (A) and hydrodynamic voltammogram for DA detection using rGO-PtNP-CB/Tyr SPCEs with 100 μM DA in 0.1 M PBS (pH 7.2).

Fig. 4(A). The amperometric results show a similar trend which was found in the cyclic voltammetric experiments. As can be seen in Fig. 4(A), the rGO-PtNP-CB/Tyr composite modified SPCEs shows the highest response to DA compare with other three SPCEs. This signal enhancement also explained the synergistic effect of rGO, PtNP and CB as described in the cyclic voltammetric studies.

3.3. Optimization of experimental parameters

In order to obtain the optimal electrode performance, experimental parameters such as pH and operation potential, are optimized. Hydrodynamic voltammetric measurements were carried out to determine the optimum operation potential for the detection of DA. Fig. 4(B) shows the amperometric response for 100 μM DA using an rGO-PtNP-CB/Tyr. SPCE with applied potentials ranged from -0.6 V to 0.1 V *vs.* Ag/AgCl. The maximum current response of the electrode was obtained at the potential from 0 V to -0.1 V. When the potential was further changed negatively up to -0.6 V, the response current was gradually decrease and the background current was significantly increased due to the reduction of dissolved oxygen. After this consideration, -0.1 V was chosen as an operating potential and all further experiments were performed at the same potential. At this potential, in addition, the possible chemicals presence in real samples such as AA, UA, NorEP, EP, L-DOPA, SR and DOPAC could not interfere the electrochemical reduction of DA. The effect of operating pH was also investigated by using 100 μM DA prepared in PBS with pH ranged from 6.0 to 7.4. The current responses increase with increasing pH up to 7.2 and then it decreases as pH increases further. This could be caused by the decay of enzyme activity in the alkaline pH.[34] At pH 7.2, the reproducibility of the SPCES to DA also shows the maximum value. These results could demonstrate that the immobilization procedure did not alter the activity of enzyme. Consequently, the optimum operating pH was chosen as pH 7.2 and all subsequent experiments were carried out at this pH.

3.4. Calibration curves of nano-composite biosensor to DA

Fig. 5 shows representative calibration curves

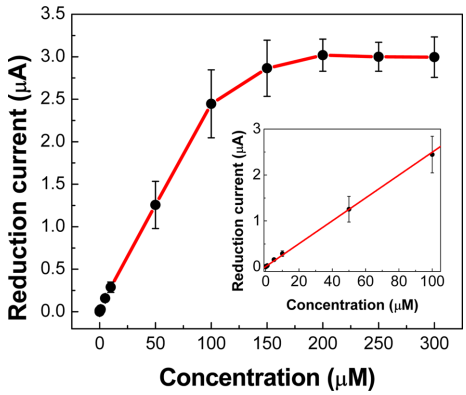

Fig. 5. Calibration curves for DA using rGO-PtNP-CB/Tyr SPCEs, experimental condition was same as described in Fig. 4B.

obtained from the results of amperometric measurements of DA by using rGO-PtNP-CB/Tyr SPCEs under the optimized experimental conditions. The aliquots of DA samples were prepared in PBS and the sample concentration was ranged from 10 nM to 300 μM. The inset in Fig. 5 shows a calibration plot of DA and each error bar indicates a standard deviation obtained from five measurements of each point. In the plot constructed, a linear range was found to be from 10 nM to 100 μM and current varies as i (μA) = 0.025 (μA) DA concentration (μM) + 0.005 (μA) with correlation coefficient (R^2) of 0.9601. The lower detection limit of rGO-PtNP-CB/Tyr SPCEs was calculated as 14 nM from blank tests. The sensitivity of rGO-PtNP-CB/Tyr SPCEs was also calculated to be 0.4 $\mu A \mu M^{-1} cm^{-2}$ and the sensor performance exhibits a good reproductively with a relative standard deviation (RSD) of 8.7 %.

3.5. Interference studies

Some chemicals are common in real biological samples that could interfere electrochemical DA detections such as AA, UA, NorEP, EP, L-DOPA, SR and DOPAC. In order to evaluate the selectivity of the rGO-PtNP-CB/Tyr SPCEs, a series of amperometric measurements were carried out by using the same procedure described in the Section 3.4. In Fig. 6, the amperometric results of the rGO-PtNP-CB/Tyr SPCEs were shown with the consecutive addition of 200 μM AA, 200 μM UA, 100 μM SR, 50 μM L-DOPA, 10 μM NorEP, 10 μM EP and 50 μM DOPAC. There were no detectable amperometric responses of the rGO-PtNP-CB/Tyr SPCEs were observed after the addition of AA, UA, SR, NorEP or EP while the same sensor showed a well-defined amperometric response to 5 μM DA (99.71 $nA\mu M^{-1}$). Detectable current responses were observed with of L-DOPA (17 $nA\mu M^{-1}$) and DOPAC (7.3 $nA\mu M^{-1}$). The current responses to the precursor of DA (L-DOPA) and DA metabolite (DOPAC) could be ascribed to their similar structure to DA and their interference were a common problem in electrochemical DA sensor systems.[35] It is apparently noted that L-DOPA and DOPAC could be interfere the sensor performance. However, their much lower sensitivities to the sensor and relatively lower concentration level in real samples[35] compared with the values of DA, could overcome this interference related limitation.

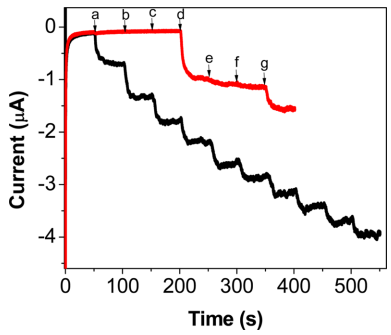

Fig. 6. Amperometric responses (red line) showing the selectivity of rGO-PtNP-CB/Tyr SPCEs to the addition of 200 μM AA(a), 200 μM UA (b), 100 μM SR (c), 50 μM L-DOPA (d), 10 μM NorEP (e), 10 μM EP (f) and 5 μM DOPAC (g). Amperometric response (black line) of rGO-PtNP-CB/Tyr SPCEs to the additions of 5 μM dopamine. experimental condition was same as described in Fig. 4B.

4. Conclusions

This study introduces the use of new nano-composite carbon inks for the fabrication of disposable screen printed dopamine sensors. The composition of nano-composite ink was characterized by XPS and the biocompatible matrix, chitosan, was successfully integrated for the enzyme, tyrosinase, immobilization. It is demonstrated that the synergetic effect of integrated rGO and PtNP in the nano-composite, clearly enhances electro-catalytic activity of the rGO-PtNP-CB/Tyr SPCEs for the detection of DA. It is, however, suggested that further optimization could be required to eliminate the interference from L-DOPA and DOPAC. The simple screen-printing technique and the effective one step sensor modification procedure using direct printing the nano composite on the surface of the SPCEs allows inexpensive disposable sensor manufacture which could be applied for mass-production. Finally, the real-time detection of DA in clinical or biological samples are currently under investigation.

Acknowledgements

This work was supported by a 2-Year Research Grant of Pusan National University.

References

1. W. Schultz, *Annu Rev Neurosci*, **30**, 259-288 (2007).
2. M. Perry, Q. Li and R. T. Kennedy, *Anal. Chim. Acta*, **653**(1), 1-22 (2009).
3. F. Musshoff, P. Schmidt, R. Dettmeyer, F. Priemer, K. Jachau and B. Madea, *Forensic Sci. Int.*, **113**(1-3), 359-366 (2000).
4. A. El-Beqqali, A. Kussak and M. Abdel-Rehim, *J. Sep Sci*., **30**(3), 421-424 (2007).
5. T. Yoshitake, J. Kehr, K. Todoroki, H. Nohta and M. Yamaguchi, *Biomed. Chromatogr.*, **20**(3), 267-281 (2006).
6. A. Kankaanpaa, E. Meririnne, K. Ariniemi and T. Seppala, *J. Chromatogr. B*, ***753***(2), 413-419 (2001).
7. L. Zhang, N. Teshima, T. Hasebe, M. Kurihara and T. Kawashima, *Talanta*, **50**(3), 677-683 (1999).
8. K. Jackowska and P. Krysinski, *Anal. Bioanal Chem*., **405**(11), 3753-3771 (2013).
9. D. L. Robinson, A. Hermans, A. T. Seipel and R. M. Wightman, *Chem. Rev*., **108**(7), 2554-2584 (2008).
10. S. R. Ali, Y. Ma, R. R. Parajuli, Y. Balogun, W. Y. Lai and H. He, *Anal. Chem*., **79**(6), 2583-2587 (2007).
11. C. F. Tang, S. A. Kumar and S. M. Chen, *Anal. Biochem*, **380**(2), 174-183 (2008).
12. S. Ku, S. Palanisamy and S. M. Chen, *J. Colloid Interface Sci*., **411**, 182-186 (2013).
13. Y. L. Zhou, R. H. Tian and J. F. Zhi, *Biosens Bioelectron*, **22**(6), 822-828 (2007).
14. J. Huang, Y. Liu, H. Hou and T. You, *Biosens Bioelectron*, **24**(4), 632-637 (2008).
15. K. Min and Y. J. Yoo, *Talanta*, **80**(2), 1007-1011 (2009).
16. M. Zhou, Y. Zhai and S. Dong, *Anal. Chem.*, **81**(14), 5603-5613 (2009).
17. M. Moreno, A. S. Arribas, E. Bermejo, M. Chicharro, A. Zapardiel, M. C. Rodriguez, Y. Jalit and G. A. Rivas, *Talanta*, **80**(5), 2149-2156 (2010).
18. K. S. Prasad, G. Muthuraman and J. M. Zen, *Electrochem. Comm.*, **10**(4), 559-563 (2008).
19. J. Ping, J. Wu, Y. Wang and Y. Ying, *Biosens Bioelectron*, **34**(1), 70-76 (2012).
20. A. Salimi, V. Alizadeh and R. G. Compton, *Analytical Sci.*, **21**(11), 1275-1280 (2005).
21. T. Kuila, S. Bose, P. Khanra, A. K. Mishra, N. H. Kim and J. H. Lee, *Biosens Bioelectron*, **26**(12), 4637-4648 (2011).
22. Z. Liu, B. Liu, J. Kong and J. Deng, *Anal. Chem*., **72**(19), 4707-4712 (2000).
23. Y. C. Tsai and C. C. Chiu, *Sensor. Actuat. B-Chem.*, **125**(1), 10-16 (2007).
24. E. S. Forzani, G. A. Rivas and V. M. Solis, *J. Electroanal. Chem.*, **435**(1-2), 77-84 (1997).
25. S. Tembe, B. S. Kubal, M. Karve and S. F. D'Souza, *Anal. Chim. Acta*, **612**(2), 212-217 (2008).
26. Y. Wang, X. Zhang, Y. Chen, H. Xu, Y. Tan and S. Wang, *Am. J. Biomed. Sci.*, **2**(3), 209-216 (2010).
27. S. C. Chang, K. Rawson, C. J. McNeil, *Biosens Bioelectron*, **17**(11-12), 1015-1023 (2002).
28. M. R. Montereali, L. Della Seta, W. Vastarella and R. Pilloton, *J. Mol. Catal. B: Enzym.*, **64**, 189-194 (2010).
29. R. Solna, E. Dock, A. Christenson, M. Winther-Nielsen, C. Carlsson, J. Emneus, T. Ruzgas and P. Skladal, *Anal. Chim. Acta*, **528**(1), 9-19 (2005).
30. W. S. Hummers and R. E. Offeman, *J. Am. Chem. Soc.*, **80**(6), 1339-1339 (1958).
31. S. Stankovich, D. A. Dikin, R. D. Piner, K. A. Kohlhaas, A. Kleinhammes, Y. Jia, Y. Wu, S. T. Nguyen and R. S. Ruoff, *Carbon*, **45**(7), 1558-1565 (2007).
32. Y. Wang, J. Liu, L. Liu and D. D. Sun, *Nanoscale Res Lett*., **6**(1), 241 (2011).
33. W. Qin and X. Li, *J. Phys. Chem. C*, **114**(44), 19009-19015 (2010).
34. T. E. Barman, 'Enzyme Handbook', Vol. 1, Springer, New york, 1969.
35. J. Njagi, M. M. Chernov, J. C. Leiter, S. Andreescu, *Anal. Chem*., **82**(3), 989-996 (2010).